JACS
JOURNAL OF THE AMERICAN CHEMICAL SOCIETY

ARTICLE

pubs.acs.org/JACS

Correlation of CdS Nanocrystal Formation with Elemental Sulfur Activation and Its Implication in Synthetic Development

Zheng Li,[†] Yijing Ji,[‡] Renguo Xie,[†] Susan Y. Grisham,[†] and Xiaogang Peng*[,†,‡]

[†]Department of Chemistry and Biochemistry, University of Arkansas, Fayetteville, Arkansas 72701, United States

[‡]Department of Chemistry, Zhejiang University, Hangzhou 310027, P. R. China

Supporting Information

ABSTRACT: Formation of CdS nanocrystals in the classic approach (with octadecene (ODE) as the solvent and elemental sulfur and cadmium carboxylate as the precursors) was found to be kinetically dependent on reduction of elemental sulfur by ODE, which possessed a critical temperature (~180 °C). After elemental sulfur was activated by ODE, the formation reaction of CdS followed closely. 2-tetradecylthiophene from the activation of S by ODE and fatty acids from the formation reaction of CdS were found to be the only soluble side products. The overall reaction stoichiometry further suggested that oxidation of each ODE molecule generated two molecules of H_2S, which in turn reacted with two molecules of cadmium carboxylate molecules to yield two CdS molecular units and four molecules of fatty acids. In comparison to alkanes, octadecene was found to be substantially more active as a reductant for elemental sulfur. To the best of our knowledge, this is the first example of quantitative correlation between chemical reactions and formation of high-quality nanocrystals under synthetic conditions. To demonstrate the importance of such discovery, we designed two independent and simplified synthetic approaches for synthesis of CdS nanocrystals. One approach with its reaction temperature at the critical temperature of S activation (180 °C) used the same reactant composition as the classic approach but without any hot injection. The other approach performed at an ordinary laboratory temperature (≤100 °C) and in a common organic solvent (toluene) was achieved by addition of fatty amine as activation reagent of elemental sulfur.

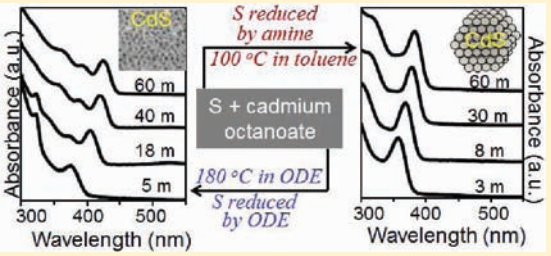

INTRODUCTION

Studies on formation mechanism of nearly monodisperse colloidal nanocrystals have attracted substantial attention in the field of chemistry because of their great potential as functional materials and interesting model systems for fundamental research.[1,2] Although formation of nanocrystals should be a typical crystallization process, there are often some chemical reactions needed to take place prior to the crystallization process. This is so because the field is actively pushing toward "greener" synthetic chemistry,[3] which often requires synthesis starts with precursors that need to be converted to reactive "monomers" for the nucleation and growth of the targeted nanocrystals. For instance, for the most studied high-quality chalcogenide nanocrystals (including II−VI, IV−VI, and I−III−VI semiconductor nanocrystals), elemental sulfur, selenium, and tellurium dissolved in organic solvents (such as octadecene and organophosphines) are commonly used as the chalcogenide precursors.[4,5] These elements (S^0, Se^0, and Te^0) must be reduced into a certain form, and then they can bond with the necessary cations to form the targeted semiconductor nanocrystals. As a result, the mechanistic studies on formation of high-quality semiconductor nanocrystals have been focused on two separated fronts. Along the first front, kinetics of formation of nanocrystals, especially their size and shape evolution, has been studied extensively in the past 20 years.[1,2] On the second front, studies on the related chemical reactions and molecular mechanisms have become active recently.[6−26] Although molecular mechanism studies might be carried out with crystallization kinetics in the background,[10,19,21,27] the correlation between these two fronts has not been clearly identified yet. Understanding of such correlation is not only important for establishing much needed quantitative framework for crystallization but also shall further shed new light on development of synthetic chemistry for high-quality nanocrystals as to be demonstrated in this report.

The II−VI semiconductor nanocrystals, especially CdSe and CdS, were established as the first examples of high-quality colloidal nanocrystals among all types of colloidal nanocrystals.[4,5] As fundamental model systems, their well-defined size-dependent optical properties due to quantum confinement[28] offer convenient probes for the mechanistic studies on formation of nanocrystals. Equally important, active exploration of technical applications of colloidal nanocrystals in both academic and industrial settings has been mostly centered on II−VI semiconductor nanocrystals at present.

The commonly adopted synthetic methods for high-quality CdSe and CdS nanocrystals in the field are typically performed

Received: May 18, 2011
Published: September 22, 2011

dx.doi.org/10.1021/ja204538f | J. Am. Chem. Soc. 2011, 133, 17248–17256

under temperatures roughly in the range between 200 and 300 °C.[5,29,30] Studies on the molecular reaction mechanisms for CdSe nanocrystals in both coordinating solvents[9] and noncoordinating solvents[7,9,11,19,22] have been reported extensively in the past several years. Very recent reports further indicate that formation of high-quality CdSe nanocrystals using Se dissolved in organophosphines as the Se precursor was largely associated with and controlled by the structure and activation of the Se−phosphine precursors.[19,21,22] These studies revealed that, in both types of media, the chemical reactions involved in formation of CdSe nanocrystals are quite different from what was originally hypothesized. Although such insights have not been incorporated into new synthetic development yet, they certainly helped us to understand the chemical complexity during formation of high-quality CdSe nanocrystals. Conversely, to the best of our knowledge, molecular mechanisms for formation of high-quality CdS nanocrystals has not been explored though the classic synthetic approach of high-quality CdS nanocrystals was introduced into the field along with the noncoordinating solvent approach about 10 years ago.[29] The different status between CdSe and CdS systems is partially because one might think that the molecular reaction mechanism for formation of CdSe and CdS nanocrystals with similar precursors in a similar solvent system, such as the common noncoordinating solvent octadecene (ODE), would be similar. The results to be described below shall actually reveal that this was not the case.

In this report, we chose CdS nanocrystals as the main model system to explore the correlation between formation of the nanocrystals and the key chemical reaction (or the rate-determining reaction step). The chemical reactions involved and formation of nanocrystals shall both be explored quantitatively or semiquantitatively for clarification of the correlation. The results described below shall reveal that the reduction of elemental sulfur by ODE, instead of nucleation of the nanocrystals, was likely the rate-limiting step for synthesis of high-quality CdS nanocrystals. To verify this conclusion, a noninjection synthetic approach was designed and examined, which yielded CdS nanocrystals with similar quality. Furthermore, by activation of elemental sulfur with fatty amines, formation of good quality CdS nanocrystals at much reduced reaction temperature, ~100 °C in comparison to ~250 °C in the classic approach, using a common organic solvent (toluene) was achieved. Success on growth of good quality CdS nanocrystals using typical laboratory temperatures and solvents not only further confirms the determining role of activation of the S precursor on formation of CdS nanocrystals but also paves the way for removing the high-temperature requirement and exotic solvents in high-quality colloidal nanocrystal synthesis.

RESULTS AND DISCUSSION

Three Synthetic Schemes. Three distinguishable but related reaction schemes were adopted and developed in this work. In the first synthetic system, CdS nanocrystals were formed by injection of elemental sulfur dissolved in octadecene (ODE) into a hot solution of cadmium fatty acid salts in ODE at a given reaction temperature (see details in Experimental Section). This scheme was introduced into the field in 2002[29] and will be called as the classic synthetic approach for the sake of presentation in this report.

The second reaction scheme did not involve any hot injection, but used the same precursors and solvent as the classic approach,

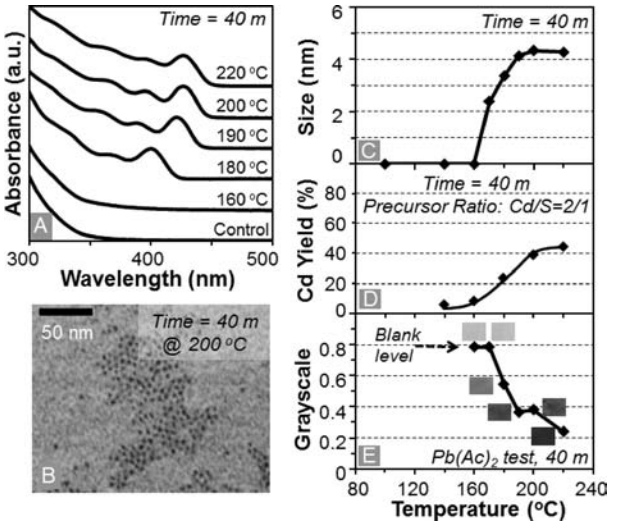

Figure 1. (A) Temperature dependence of formation of CdS nanocrystal, UV−vis spectra taken at 40 min for each reaction. (B) TEM image of CdS nanocrystal grown at 200 °C for 40 min. (C) Temperature-dependent particle size of CdS nanocrystals at 40 min. (D) Cd precursor conversion ratio (Cd yield) for the reactions at different temperatures. (E) Images and grayscale plot of lead acetate ($Pb(Ac)_2$) testing papers for H_2S detection after 40 min exposure to the reaction atmosphere under different temperatures (no cadmium precursor in the reaction flask).

which will be called as the noninjection approach in this report. Such a noninjection synthetic approach was formulated after identification of the rate-determining step, activation of elemental sulfur at a given temperature range, in the first system.

The third reaction system was designed to explore synthesis of CdS nanocrystals at a typical laboratory temperature (≤100 °C) in a regular solvent (such as toluene). This reduced temperature approach was also designed to further confirm the activation of elemental sulfur as the key chemical reaction in the formation of CdS nanocrystals by the addition of aliphatic amine, which is known to be a strong activation reagent for elemental sulfur.

Temperature Dependence of Formation of CdS Nanocrystals in the Classic Synthetic Scheme. Experiments were carried out to identify temperature effects for formation of CdS nanocrystals using the classic synthetic approach in the temperature range between about 100 and 220 °C. The temperatures used here were somewhat lower than that used in the original synthetic scheme (typically >250 °C).[29] Some preliminary results reported recently by us indicated that formation of high-quality CdS nanocrystals comparable to the classic approach using the same reaction system could occur at a temperature below 250 °C,[27] and the preliminary data further implied that formation of CdS nanocrystals in this classic approach was likely controlled by a chemical kinetic process, instead of a nucleation process. These preliminary results served as an initial base for us to design the experiments for this part of the research.

Figure 1A illustrates the UV−vis absorption spectra of the aliquots taken from the reaction mixtures carried out at a given temperature. All reactions were performed with identical chemical composition, and the only difference among these reactions was the reaction temperature (marked in Figure 1A). When the aliquots were taken for recording the spectra, each reaction proceeded for 40 min after injection of the sulfur solution. Results clearly revealed that for the reactions with reaction temperature

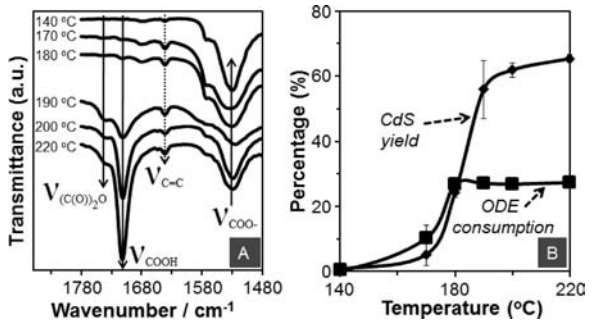

Figure 2. (A) Evolution of FT-IR spectra of the mixture of $Cd(Oc)_2$, ODE, and elemental sulfur at different reaction temperatures. (B) Consumption of ODE determined by NMR measurements and CdS yield measured by the conversion ratio of elemental sulfur for a series of reactions (initial $Cd(Oc)_2$/ODE/elemental sulfur = 1:1:1) at different reaction temperatures.

below about 170 °C, the absorption spectrum of the aliquots (see the spectrum for 160 °C reaction in Figure 1A) resembled that of the mixture of the starting materials (see the spectrum marked as "control" in Figure 1A). This indicates that, at this relatively low temperature range, no formation of CdS nanoclusters/nanocrystals was observable by UV−vis spectra after the reactants aged for 40 min.

Conversely, when the reaction temperature was above 170 °C, formation of nearly monodisperse CdS nanocrystals was observed under the same reaction conditions, which was indicated by the sharp absorption features in each spectrum (Figure 1A). The quality of the nanocrystals was about the same as that obtained in the classic scheme carried out in the temperature range between 250 and 300 °C,[29] with similar sharp absorption features, nearly pure bandgap photoluminescence, and narrow size distribution with dot-shape (see a transmission electron microscope (TEM) image in Figure 1B as an example).

The average size of the CdS nanocrystals in the 40-min aliquots for each reaction was determined using the absorption peak position,[31] which showed a sharp increase upon increase of the reaction temperature in the range approximately between 170 and 200 °C (Figure 1C). The Cd conversion ratio (Figure 1D) from the Cd precursor to CdS units in nanocrystals (Cd yield) determined using the so-called "Cadion" colorimetric method (see Experimental Section and Supporting Information for details) showed a similar increase trend in this temperature range. A gravimetric analysis for CdS unit yield for a more concentrated reaction (Figure 2 and see details below) also demonstrated a similar trend seen in Figure 1D.

These results imply that formation of CdS nanocrystals occurred rather abruptly after the system reached a critical temperature, ~180 °C. The existence of a critical temperature in Figure 1C might be due to a thermally activated chemical reaction at this temperature. This is consistent with the preliminary results reported recently by us, that formation of CdS nanocrystals in the classic approach was controlled by a chemical kinetic process instead of nucleation kinetics.[27]

The Cd yield data identified under synthetic conditions (Figure 1D) are important to reveal the reaction stoichiometry for formation of CdS nanocrystals. The data sets presented in Figure 1, specifically including Figure 1D, were collected for the reaction with oleic acid as the ligands for both Cd precursor and nanocrystals (see "typical synthesis" in Experimental Section). The results indicate that this trend was quantitatively reproducible with either oleic acid or a saturated fatty acid as the ligands. However, the accuracy of the Cd yields measured by the Cadion method largely depended on the purification of the CdS nanocrystals from the other metal-containing impurities, that is, Cd fatty acid salts in our case. Using a new purification procedure (see Experimental Section), it was possible to remove unreacted Cd fatty acid salts quantitatively (see FTIR spectra in Figure S1, Supporting Information). It should be mentioned that our results indicate that the Cd yields calculated using the extinction coefficients of CdS nanocrystals published previously[31] were only qualitatively correct, which is possibly due to two reasons, namely, the biased Cd ion concentration from unpurified Cd fatty acid salts in the measurements of the original extinction coefficients and the excess Cd ions on the surface of nanocrystals (see discussions below).

Rate-Determining Chemical Reaction in Formation of CdS Nanocrystals. Experiments were performed to identify possible chemical reaction(s) that might match the critical temperature discussed in the above paragraph. Cadmium fatty acid salts alone, pure ODE, and mixtures of cadmium fatty acids salts with the corresponding fatty acids and ODE, if no elemental sulfur existed in the solution, were found to be stable in the experimental temperature range. No changes were identified by UV−vis, FTIR, and NMR measurements. Conversely, significant changes were detected upon heating the mixture of elemental sulfur and ODE, without any cadmium precursors, in the temperature range of interest by several experimental techniques.

Figure 1E shows the results of lead acetate ($Pb(Ac)_2$) tests for H_2S detection by applying $Pb(Ac)_2$ testing paper strips to the reaction atmosphere above the mixture of elemental sulfur and ODE. It reveals that the testing paper strips were colorless at low temperatures and they turned black at temperature above 170 °C due to the formation of black lead sulfide. The general trend of the grayscale plot of this test matched well with the trend for the formation of CdS nanocrystals when the cadmium precursors, cadmium fatty acid salts, were in place (comparing Figure 1C,D with Figure 1E). The gas phase mixture from the reactions without cadmium precursors was also bubbled into silver nitrate and zinc acetate solutions separately. The colorless silver nitrate and zinc acetate solutions became black and white suspensions, respectively, implying the formation of black silver sulfide and white zinc sulfide. These results all indicate the generation of H_2S gas by reacting elemental sulfur with ODE.

$$S + CH_3(CH_2)_{15}CH{=}CH_2 \rightarrow H_2S + \text{side product(s)} \quad (1)$$

The nice correlation between the plots in the right panel of Figure 1 suggests that this reaction is likely the rate-determining step for the formation of CdS nanocrystals. This will be verified in the following subsection. Furthermore, in reaction 1, we did not specify the nature of side products, which will also be discussed in the following subsection.

Chemical Reactions Involved in Formation of CdS Nanocrystals. Results in Figure 1 imply that formation of CdS nanocrystals is likely initiated by the activation of elemental sulfur. To confirm this hypothesis and identify the reaction stoichiometry, reactions with an equal molar amount of cadmium octanoate ($Cd(Oc)_2$), ODE, and elemental sulfur were carried out (Figure 2). The results in the above subsection indicate that ODE can react with elemental sulfur to generate H_2S gas. When a

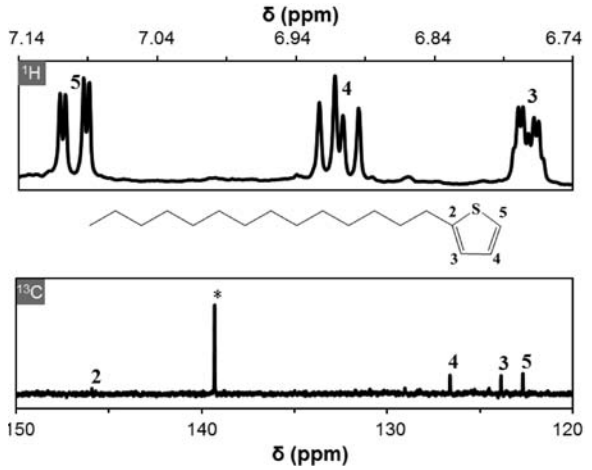

Figure 3. ^{1}H and ^{13}C spectra of the final products at 220 °C after HCl digestion. The peak with asterisk on the ^{13}C spectrum comes from the carbon at the 2 position of 1-octadecene.

sufficient amount of cadmium fatty acid salts were in the reaction mixture, however, H_2S gas became undetectable using the same methods mentioned in the above subsection. Instead, formation of CdS nanocrystals was observed presumably by the rapid reaction of H_2S with cadmium fatty acid salts presented in the reaction solution. If this reaction did take place, one of the side products should be fatty acid. FTIR measurements indeed revealed formation of fatty acid (Figure 2A), which could not be observed without the presence of elemental sulfur as mentioned above. Furthermore, FTIR results revealed that formation of free fatty acid occurred in a similar temperature range (Figure 2A) as the formation of H_2S shown in Figure 1E. In addition to formation of the fatty acid, a trace amount of the corresponding anhydride was also detected by FTIR (Figure 2A),[32] which presumably should be the product of dehydroxylation of the fatty acids upon prolongated heating. Ignoring the existence of this trace amount of anhydride, one can write the main reaction for formation of CdS as follows (using cadmium octanoate ($Cd(Oc)_2$) as the cadmium precursor).

$$H_2S + Cd(Oc)_2 \rightarrow CdS + 2HOc \quad (2)$$

In principle, if reaction 2 was fast enough, formation of CdS through reaction 2 should follow reaction 1 closely. To further verify the correlation between reactions 1 and 2, quantitative studies were carried out at different temperatures with an equal molar amount of $Cd(Oc)_2$, ODE, and elemental sulfur, namely, the ones shown in Figure 2. Here, reaction 1 was measured by the consumption of ODE in the final products, which was determined using the α-H NMR peak of its C=C double bond. For a given final products, reaction 2 was quantitatively monitored using the unit yield of CdS in solid form through gravimetric analysis (see Experimental Section for details). The quantitative results are shown in Figure 2B, which first confirmed that the temperature dependence of both reactions were consistent with the trend shown in the right panel of Figure 1. Second, for a reaction started with $Cd(Oc)_2$/ODE/S = 1:1:1 (molar ratio), the ultimate yield of CdS units was about twice the consumption of the ODE (see the plateau values for two curves in Figure 2B), which means that

$$(\text{yield of CdS})/(\text{consumption of ODE}) = 2:1 \quad (3)$$

Importantly, (yield of CdS)/(consumption of ODE) was found to be almost the same even if the reaction proceeded for 60 min at a relatively high temperature, namely 220 °C. From the stoichiometry of the reaction mixture, because the ultimate consumption of ODE was about 33% (See Figure 2B), one can further calculate that

$$(\text{consumption of S})/(\text{consumption of ODE}) = 3:1 \quad (4)$$

As discussed above, both ODE consumption and CdS yield showed an ultimate value, indicated by the plateau in both curves in Figure 2B. Two facts supported that the ultimate yield of CdS at relatively high temperatures in Figure 2 was likely due to the total consumption of elemental sulfur. First, NMR measurements indicate that there was plenty of ODE left (see ^{13}C NMR in Figure 3 and Figure S2, Supporting Information) when the reactions reached plateau in Figure 2B. Second, given the initially equal molar amount of ODE and S, consumption of elemental sulfur was about three times of ODE (eq 4 and Figure 2B).

As ultimate yield of S in the form of CdS was only 2/3 of the initial elemental sulfur, some elemental sulfur should be consumed by formation of inactive side product(s) in reaction 1. For the reaction with $Cd(Oc)_2$/ODE/S = 1:1:1, the final products were digested by using concentrated HCl to decompose CdS completely, and $CdCl_2$ was removed by extraction (see Experimental Section for details). The oxidation product of ODE in the organic phase could be divided into two portions. The first portion was typically black in color and not soluble in common organic solvents tested, and analysis of the chemical structure was not successful. The second portion was identified as 2-tetradecylthiophene (see the molecular structure as an inset in Figure 3). Because the thiophene molecule has a S atom, the conversion ratio of elemental sulfur could not be 100%, supporting elemental sulfur as the limiting reagent. Further quantitative analysis reveals that this oxidation product of ODE in the second portion accounted for about ~13% of total CdS yielded under a general synthesis condition (Figure S3, Supporting Information). With this result, we write the following reaction at least as a part of reaction 1:

$$3S + CH_3(CH_2)_{15}CH{=}CH_2 \rightarrow 2H_2S + CH_3(CH_2)_{13}(C_4H_3S) \quad (5)$$

It should be emphasized that reaction 5 was based on the existence of the 2-tetradecylthiophene as the only S-containing side product in the soluble portion of the organic residue. However, it is interesting to notice that, although reaction 5 was established by the soluble portion of the oxidation products of ODE, it gave a 3:1 consumption ratio between elemental sulfur and ODE. Evidently, this number is consistent with eq 4, which was deduced with a different set of experimental evidence (see the text above eq 4). This led to a conclusion that the overall activation reaction of elemental sulfur by ODE, namely, reaction 1, should give a similar set of reaction coefficients for the reactants (ODE and S) although we could not identify the exact structure(s) of the side product(s) in the insoluble portion.

The exact structure of 2-tetradecylthiophene was identified by NMR (Figure 3), gas chromatography−mass spectroscopy (GC-MS, Figure 4), and $^{1}H-^{13}C$ HMQC (heteronuclear multiple

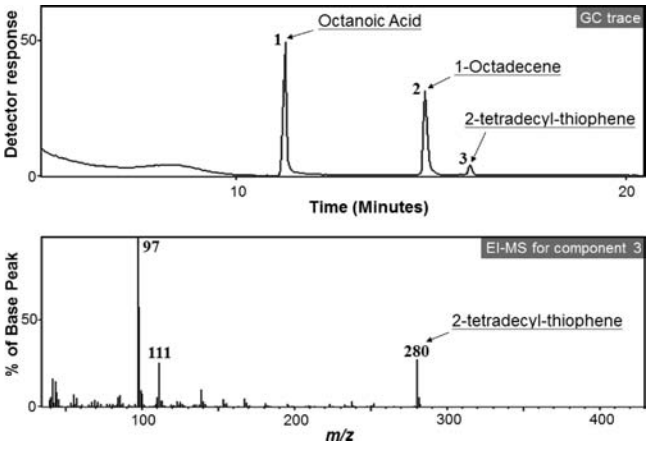

Figure 4. Gas chromatography (GC) of the final products after digestion by HCl and the electron ionization mass spectrum (EI-MS) of the third component in the GC trace.

quantum correlation, Figure S4 in Supporting Information). The final products were analyzed using GC-MS after digestion by concentrated HCl and removal of water-soluble species including all inorganic ions. The GC trace in Figure 4 (top) indicates that there are three organic components in the reaction mixture. The identification of the chemical composition for each component was provided by the following electron ionization mass spectrum (EI-MS). The first and second components were determined as octanoic acid, converted from cadmium fatty acid salt through either reaction 2 or the digestion process, and ODE (see their EI-MS in Figure S5, Supporting Information), respectively.

The EI-MS spectrum of the third component (Figure 4, bottom) is consistent with tetradecylthiophene. The molecular ion peak located at 280 confirmed the existence of tetradecylthiophene. The small peak at 281 could be assigned as a result of the natural abundance of the elements. The EI-MS peaks at 111 and 97 series with 14 mass units apart for the third component could be assigned to the fragmented tetradecyl alkane chain with one CH_2 difference in mass. These results indicate that the GC-MS experiments confirmed the assignment of the structure of tetradecylthiophene and supported the reactions involved in formation of CdS nanocrystals (reactions 1, 2, and 5). While GC-MS experiments offered molecular formula information about the molecule suspected to be tetradecylthiophene, $^{1}H-^{13}C$ HMQC and the analysis (Figure S4, Supporting Information) indicate that its structure is consistent with the molecular structure of 2-tetradecylthiophene.

Various characterization techniques including NMR, FTIR, and GC-MS did not show any sign of thiol or disulfide during the synthesis of CdS nanocrystals, although their counterparts were observed in the case of formation of CdSe nanocrystals using a similar reaction system.[22] Furthermore, the Se version of the identified oxidation product of S observed in this work (2-tetradecylthiophene) had not been reported for formation of CdSe nanocrystals using a similar reaction system.[9,11,22]

The existence of the double bond presumably made the α and β hydrogens reactive for oxidative elimination in ODE. With elemental sulfur in place, this further induced the formation of 2-tetradecylthiophene as the final oxidation product in reaction 5. Nonexistence of other types of S-containing side products as mentioned in the above paragraph further indicates that the saturated hydrocarbon chain of octadecene could not compete with the α and β hydrogens of the double bond. It should be pointed out that, reduction of S by hydrocarbons to form thiophenes as redox products was mentioned in some books.[33−35]

However, it is well-known that elemental sulfur can react with alkane under elevated temperatures to generate many types of S-containing and complex products.[33−36] Therefore, in order to examine the unique properties of the double bond in ODE for activating elemental sulfur in the classic synthetic approach of CdS nanocrystals,[29] experiments were attempted to use high boiling point alkane as the solvent. The results indicate that formation of CdS nanocrystals could be achieved in such a saturated hydrocarbon solvent. However, even if the resulting CdS nanocrystals were quite small, the resulting reaction solution was brown to black in color, instead of colorless (bright yellow for large CdS nanocrystals) reaction solution obtained in ODE (Figure S6, Supporting Information). Consistent with this, the typical UV−vis spectra of the CdS nanocrystals formed in high boiling point alkane showed a significant scattering background (Figure S6, Supporting Information). With these facts, one could conclude that ODE, in comparison with saturated hydrocarbons, is a preferred reducing reagent (solvent) for elemental sulfur due to the existence of the double bond.

Preliminary results on synthesis of PbS nanocrystals using a similar reaction system (Figure S7, Supporting Information) indicates a similar correlation pattern between activation of elemental sulfur by ODE and formation of PbS nanocrystals. Similar to the CdS nanocrystal system discussed above, formation of PbS colloidal nanocrystals was found to be abruptly activated in the temperature range between 160 and 180 °C (Figure S7, Supporting Information).

Consistency between the Reactions in Figure 1 and the Ones in Figure 2. The reactions in Figure 2 were performed with an equal molar amount of $Cd(Oc)_2$, ODE, and elemental sulfur, which made it possible to obtain a decent amount of side products for necessary characterization discussed in the above subsection. Compared with the reactions carried out under common synthetic conditions (the ones in Figure 1), the reactions in Figure 2 were with biased high concentrations of $Cd(Oc)_2$ and elemental sulfur and much less ODE. However, the results and analysis below shall reveal that the chemical reactions illustrated above are consistent for both sets of reactions.

The CdS unit yield in Figure 2B should be equal to the Cd yield for the given system because the resulting CdS was in the form of bulk and each CdS unit contains one Cd ion. For bulk CdS, the Cd to S ratio should be 1:1. Therefore, for the reactions shown in Figure 2, the corresponding Cd yield has an ultimate value at about 66%. Because the Cd to S precursor ratio was 2:1 in Figure 1, instead of 1:1 in Figure 2, this should give us about 33% as the ultimate Cd yield for the reactions in Figure 1.

The experimental value in Figure 1 is about 42% (Figure 1D). At first sight, this value seemed to be contradictory to the value discussed in the above paragraph (33%). However, because the only ligands in the reaction system were fatty acids, the surface of the nanocrystals and the ligands were connected by RCOO−Cd bonds. Consequently, this should give CdS nanocrystals with a Cd-rich surface, which is similar to that in the case of CdSe nanocrystals solely passivated with carboxylate ligands.[37] Noticing that the size of CdS nanocrystals formed at 220 °C (Figure 1A) was about 4.3 nm, one could estimate that a full monolayer of RCOO−Cd on the surface of these nanocrystals should increase the ultimate Cd yield from 33% to about 50%. This simple model obviously overestimated the amount of

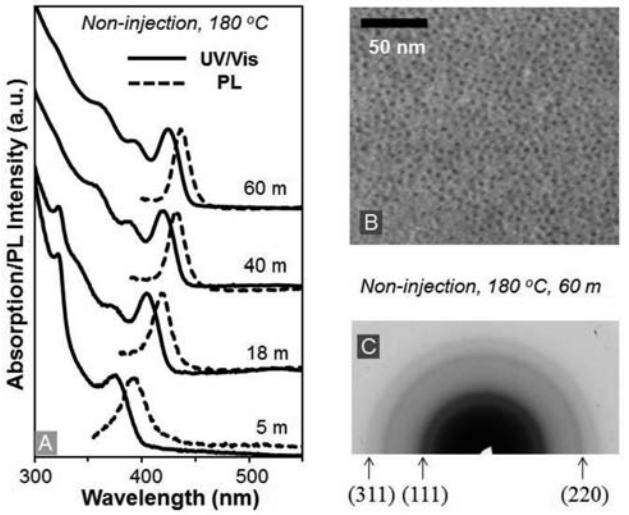

Figure 5. (A) Temporal evolution of UV−vis absorption and photoluminescence of a noninjection reaction with the final reaction temperature as 180 °C. (B) TEM image of CdS nanocrystals from a sample of the reaction shown in panel A. (C) Electron diffraction pattern of the same sample.

RCOO−Cd because the nanocrystals surface would be too crowded to accommodate a full monolayer of RCOO−Cd. With these considerations, it would be reasonable to conclude that the ultimate Cd yield based on bulk CdS (33%) and that calculated from the CdS nanocrystals (42%) are in good agreement. With the ultimate yields being consistent, we can see that the general trends in Figure 1D and Figure 2B are very similar to each other.

As for the side products identified above through the high concentration reactions in Figures 2, 3, and 4, both fatty acids (Figure S1, Supporting Information) and 2-tetradecylthiophene (Figure S3, Supporting Information) were identified for the reactions under the regular synthetic conditions. Specifically, 2-tetradecylthiophene was identified as the oxidation product of S by ODE, but there was no black insoluble substance observed under synthetic conditions.

Noninjection Synthetic Approach in ODE. The results above strongly imply that synthesis of high-quality CdS nanocrystals using the classic approach[29] involved the reduction of elemental sulfur by ODE as the rate-determining step. If this was true, the rather abrupt activation of this reaction in the temperature range between around 160 and 180 °C (Figures 1 and 2) would mean that the hot-injection step in the classic protocol[29] may not be necessary. This is so because the abrupt activation at elevated temperatures should play a similar role as a rapid injection, which should be similar to the phenomenon observed very recently for the case of Co nanocrystals.[38]

The results in Figure 5 verified the above hypothesis. All starting materials used in a typical classic approach by hot injection, namely, ODE (4 g) with 0.0674 g cadmium oleate, 0.2825 g oleic acid, and 0.0016 g S, were loaded together into the reaction flask at room temperature. The mixture was heated to 180 °C at a rate approximately 15 °C/minute. The temporal evolution of the optical properties (Figure 5A) followed a similar pattern as a hot-injection reaction at the same temperature (Figure S8, Supporting Information). The sharp absorption features and photoluminescence peak of the final product imply that the resulting nanocrystals are nearly monodisperse and of high optical quality. The nanocrystals were dot-shaped as confirmed by TEM (Figure 5B). The electron diffraction pattern (Figure 5C) indicates that the crystal structure of the resulting CdS nanocrystals was zinc-blende.

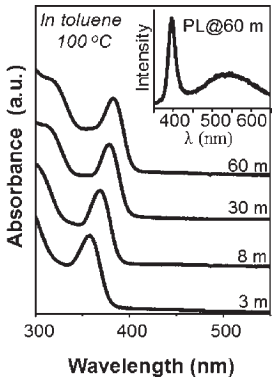

Figure 6. Temporal evolution of UV−vis absorption spectra of CdS nanocrystals grown at 100 °C in toluene. Inset is the photoluminescence (PL) spectrum of the CdS aliquots taken at 60 min.

The results in Figure 5 first supported the temperature-dependent activation of elemental sulfur revealed by studying the classic approach (Figures 1 and 2). Second, the noninjection approach could further simplify synthesis of high-quality CdS nanocrystals. It should be mentioned that noninjection synthesis of high-quality CdS nanocrystals with zinc-blende structure was reported using two different types of sulfur precursors.[39,40] Presumably one sulfur precursor was in place for nucleation and the other for growth. In addition, the reaction temperatures used in those reports were in the range of 220 and 300 °C, which was somewhat higher than the temperature used in this report. Also at 240 °C, a very recent report showed that high-quality CdS nanocrystals could be synthesized using a noninjection approach in ODE.[41]

Reduced-Temperature Approach in Toluene. The results obtained in both the classic approach and the noninjection approach discussed above indicate that, as long as elemental sulfur could be activated, formation of CdS nanocrystals would follow closely. It has been established that elemental sulfur could be activated by basic chemicals such as amines, presumably by opening the S_8 ring.[36] Such an activation process could even occur at room temperature. These facts invited us to consider synthesis of CdS nanocrystals at a temperature range reachable with common organic solvents, such as toluene, by adding amine into the reaction system.

The relatively sharp absorption spectra in Figure 6 illustrate that good quality CdS nanocrystals indeed formed at 100 °C by addition of octylamine into the reaction system consisting of elemental sulfur, cadmium fatty acid salts, and fatty amine with toluene as the solvent (see details in Experimental Section). The temporal evolution of the UV−vis spectra of the nanocrystals resembles a typical pattern using high-temperature approaches in ODE (See Figure 5A as an example). The photoluminescence spectrum of one aliquot is shown in Figure 6 as inset, which possesses a sharp band-edge emission with a weak deep trap emission tail to the long wavelength side (Figure 6, inset). The full-width-at-half-maximum (fwhm) for the band-edge emission was found to be about 22 nm, which is comparable to a typical fwhm value of PL spectra for high-quality CdS nanocrystals synthesized using classic approach.

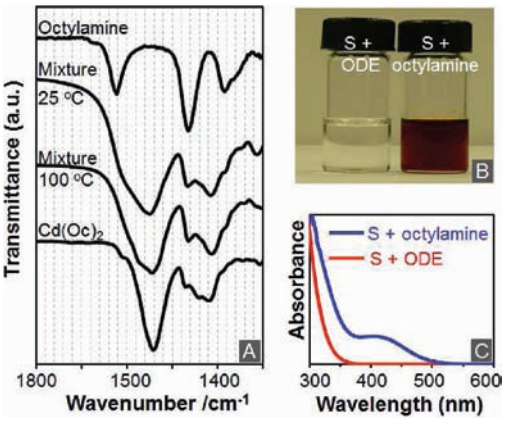

Figure 7. (A) FTIR spectra of pure octylamine, a mixture of octylamine and cadmium octanoate ($Cd(Oc)_2$) at 25 °C, a mixture of octylamine and $Cd(Oc)_2$ at 100 °C, and pure $Cd(Oc)_2$. (B) Picture of elemental sulfur in ODE and octylamine. (C) UV−vis spectra of sulfur dissolved in ODE and octylamine.

Besides addition of amine, the chain length of both fatty amine and cadmium fatty acid salts were found to be important for synthesis of CdS nanocrystals in toluene. If oleylamine and cadmium stearate were used in place of octylamine and cadmium octanoate, growth of the CdS nanocrystals was too slow to be appreciable. This was probably caused by a much reduced surface ligand dynamics on the surface of the nanocrystals at the reduced temperatures.[42] This implies that, although elemental sulfur could be activated at a common laboratory temperature, the controlled growth of high-quality nanocrystals is still dependent on other parameters needed to be optimized for a successful synthetic scheme. It should be noticed that, in a comparable temperature range, synthesis of CdS nanocrystals with somewhat lower optical quality was reported using relatively complex single precursors.[43,44] Likely because of the high reactivity of the single precursors, such as cadmium alkyl xanthates, cadmium thiocarbamates, and cadmium thiocarbonates, ligands with long hydrocarbon chains were found to be effective.

A series of experiments were carried out to further confirm that amines were indeed activating elemental sulfur, instead of activating the cadmium fatty acid salts. It is well-documented that fatty amine reacts with cadmium fatty acid salts in the case of CdSe synthesis under high temperatures (usually higher than 250 °C) to form the corresponding amides.[45] However, under the much reduced reaction temperature in this work (≤100 °C), FTIR spectra clearly revealed that no reaction occurred between fatty amine and cadmium fatty acid salts.

In Figure 7A, the FTIR spectra of the mixture of octylamine and cadmium octanoate at two different temperatures, 25 and 100 °C, are presented. For the mixture at 100 °C, it was heated at this temperature in toluene (without elemental sulfur in place) for 60 min to ensure sufficient time for any possible reaction. Evidently, both spectra of the mixtures are the superposition of the standard spectra of octylamine (top curve) and cadmium octanoate (bottom curve). In the spectra of both mixtures, there was no sign of any amide formation (see Figure S9, Supporting Information, for a standard IR spectrum of amide).

While reaction between amine and cadmium fatty acid salts in toluene did not occur, elemental sulfur easily reacted with amine. As shown in Figure 7B, at room temperature, the ODE solution of elemental sulfur is colorless, but the color of elemental sulfur dissolved in octylamine is brownish red. The color difference of two mixtures yielded two distinguishable UV−vis spectra (Figure 7C). The color and absorption features in the UV−vis spectrum of the elemental sulfur and amine mixture were assigned to the formation of sulfur radicals and open chain fragments of S due to opening of S_8 ring.[46] Recently, Ozin's group has reported a detailed account of NMR analysis of amine and elemental sulfur.[26] Our preliminary analysis of the mixture of octylamine and elemental sulfur using NMR was found to be qualitatively similar to what was reported by Ozin's group, with the formation of *N*′-octyl-2-thioketooctanamidine as possible activated products.

Although activation of elemental sulfur by amine involves much more complicated side products[26] than what was observed in sulfur activation solely by ODE (thiophene as the only detectable side product), generation of H_2S during the activation did occur in this case. Using the same testing method in Figure 1E, lead acetate testing paper also turned black for a mixture of octylamine and elemental sulfur at 100 °C, while the testing paper remained white for the octylamine without sulfur in place. Furthermore, at 100 °C, generation of H_2S during the reaction conditions was quite rapid. As a result, prevention of H_2S from evaporation was a key parameter to determine the reproducibility of this low-temperature approach. It should be pointed out that, although the proposed reaction processes between amine and elemental sulfur were complex, H_2S also appeared as one possible product in the report by Ozin's group.[26]

It should be noted that "greener" synthesis for CdSe[47] and ZnSe[48] nanocrystals in quantum confinement regime through hot-injection schemes usually needed the addition of fatty amine as an active ingredient. In contrast, using similar solvents and precursors (metal fatty acid salts and elemental chalcogens), synthetic schemes for high-quality CdS[29] and ZnS nanocrystals[48] under high temperatures (usually above 250 °C) did not need the addition of amines. In fact, amines combined with high temperatures and using elemental sulfur often made CdS and ZnS nanocrystals with poor optical performance,[49] typically with poor PL quantum yield and too large to observe quantum confinement for CdS and ZnS. The results shown here suggested that this might be a result of two related facts. One, elemental sulfur is a substantially stronger oxidant than the typical selenium precursor used, tributylphosphine−Se complex. Two, the reaction temperature used in the past for developing standard protocols for high-quality II−VI semiconductor nanocrystals was high, usually in the range between 250 and 350 °C.[29,48] As a result, if amine was in place, such high temperatures would cause elemental sulfur to be too reactive and result in a rapid growth of the sulfide nanocrystals with too large sizes to show any quantum confinement, although high temperature could be needed for activation of the selenium precursors.

CONCLUSION

In comparison to saturated hydrocarbons (alkanes), the α- and β-hydrogens in ODE were found to be sufficiently strong in a medium temperature range (~180 °C) for activation of elemental sulfur. Ultimately, there was only 2/3 of elemental sulfur could be found in the form of CdS nanocrystals, and the other 1/3 was believed to be converted into inactive organic compound, with 2-tetradecylthiophene as the only identified soluble sulfur-containing side product. The reaction stoichiometry further suggested that oxidation of each ODE molecule would generate two molecules of H_2S. As long as activation of S was in place,

formation of CdS nanocrystals would follow closely. While cadmium carboxylate salts were used as the cadmium precursor, the reactions in turn yielded carboxylic acid as the side product. Identification of the close correlation between activation of elemental sulfur and formation of CdS nanocrystals in the classic synthetic scheme enlightened us to develop a successful noninjection synthesis of high-quality CdS nanocrystals at 180 °C, using identical reactants used in a classic synthetic approach. Furthermore, by applying fatty amine as the activation reagent for elemental sulfur, we demonstrated that good quality CdS nanocrystals could be synthesized at ordinary laboratory temperatures (≤100 °C) in common organic solvents (such as toluene). These synthetic successes not only broadened and simplified the existing protocols for metal sulfide nanocrystals synthesis but also revealed the importance of understanding the relationship between the crystallization kinetics and the related molecular mechanisms.

■ EXPERIMENTAL SECTION

Materials. Cadmium oxide (CdO, Alfa), oleic acid (Aldrich), octanoic acid (Alfa), sulfur (Alfa), lead(II) acetate (Alfa), silver nitrate (Alfa), zinc acetate (Alfa), octylamine (Alfa), tetradecane (Alfa), 1-octadecene (ODE, 90%, Alfa), 1-octadecene (≥99.5%, Fluka), nitric acid (HNO_3, Zhejiang Zhongxing Chemical Reagent Co), 1-(4-nitrophenyl)-3-(4-phenylazophenyl) triazene (Cadion, Aladdin), Triton X-100 (Alfa), cadmium acetate dihydrate (Alfa), butylamine (Alfa), potassium hydroxide (KOH, Tianjin Damao Chemical Reagent Factory), chloroform (Alfa), acetone (EM Science), toluene (EM Science), D-chloroform (Alfa), methanol, ethanol, and hexanes (National Pharmaceutical Group Chemical Reagent Co) were used without further purification. All the cadmium fatty acid salts were prepared by the methods developed in our group.

Synthesis of CdS Nanocrystals. Sythesis of the CdS nanocrystals was based on the literature.[29] For a typical synthesis (reactions shown in Figure 1), 0.0128 g of cadmium oxide (0.10 mmol), 0.3390 g of oleic acid (1.20 mmol), and 3.6 g of ODE (90%) were heated to 300 °C under Ar protection until a clear solution was formed and cooled to the designated temperature in an Ar atmosphere, and then 0.0016 g of S (0.05 mmol) dissolved in 0.4 g of ODE (90%) was injected. After the injection of sulfur precursor, small aliquots were taken out at different times, diluted in the toluene solution, and measured by UV−vis.

Determination of Cadmium Precursor Conversion Ratio. The cadmium precursor conversion ratio (Cd yield) in Figure 1D was determined by a two-stage extraction technique. In the first stage, final products (0.5 mL) were mixed with 0.5 mL of hexanes and 1 mL of methanol at 50 °C to form two phases. The upper phase of this extraction system (nonpolar phase) was kept. In the second stage, extraction was repeated three times. In each extraction step, the volume of the remaining solution from the previous extraction step was increased to 1 mL by adding more hexanes; then, 20 μL of butylamine and 1 mL of methanol were added to form two phases at 50 °C. The upper solution was kept, and this procedure was repeated three times to complete the second stage extraction. FTIR spectra were applied to monitor the removal of Cd fatty acid salts (see Figure S1, Supporting Information, as examples) and UV−vis was employed to ensure the separation of CdS nanocrystals in the upper solution in each extraction step. To the final hexanes−ODE solution, acetone was added, and the turbid mixture was centrifugated at 4000 rpm for 15 min. The supernatant was decanted and 30 drops of concentrated nitric acid was added into the precipitate. The mixture was slowly heated to 300 °C to completely dissolve the sample and evaporate the remaining nitric acid. Subsequently, 20 drops of nitric acid was added and heated to 100 °C for 5 min, and DI water was added to make a 25 mL solution. The cadmium concentration in each solution was identified by comparing to the calibration curve.[50] More details are included in the caption of Figure S1, Supporting Information.

Detection of H_2S Gas. Detection of H_2S gas in Figure 1E was followed by heating elemental sulfur and 1-octadecene without cadmium precursor under Ar protection, and the gas was collected with lead acetate paper by purging through Ar. The lead acetate paper strips were collected together, and a digital picture was taken with all strips in the same shot to ensure reliable grayscale values measured in Adobe Photoshop.

Noninjection Synthesis Protocol. For the noninjection synthesis protocol, 0.0674 g of cadmium oleate (0.10 mmol), 0.2825 g of oleic acid (1.00 mmol), 0.0016 g of S (0.05 mmol) and 4 g of ODE (90%) were added into a three neck flask, bubbled with Ar for 10 min, then heated to 180 °C under Ar protection with heating ramp at around 15 °C/min.

Low-Temperature Synthesis. In a typical low-temperature synthesis, 0.0398 g of cadmium octanoate (0.10 mmol) was mixed with 8 g of toluene. After degassing at room temperature for 10 min with Ar, the solution was heated up to 100 °C under Ar protection, then 0.0008 g of S (0.025 mmol) dissolved in 0.05 mL of octylamine was injected.

Biased Precursor/ODE Ratio Reactions. The biased precursors/ODE ratio reactions used for quantitative NMR analysis, IR measurements, GC-MS, etc. were carried out as following. Equal molar amounts (2 mmol) of cadmium octanoate ($Cd(Oc)_2$), elemental sulfur, and ODE (≥99.5%) were heated under Ar protection to the designated temperature. Once the solution was heated to the specified temperature, the heating mantle was removed and then cooled to room temperature in Ar atmosphere, and 20 mL of chloroform was added into the flask. After the final products were stirred in chloroform solution for 10 min, 10 mL of 6 M HCl solution was injected into the flask, the gas was collected by silver nitrate solution. The black precipitate in the $AgNO_3$ solution was collected by centrifugation, washed through deionized water, and dried in a vacuum oven overnight. The corresponding Ag_2S weight was recorded to calculate CdS yield. The $CHCl_3$ layer in the flask was evaporated on a rotary evaporator and then added into the D-chloroform to carry out the NMR measurement. Parallel experiments were carried out under the same reaction conditions to collect the final samples for IR characterization.

To confirm that the final products from biased precursor ratio was indeed formed for routine reaction conditions, the following experiments were carried out for corresponding NMR analysis in Figure S3, Supporting Information: 0.0398 g of cadmium octanoate (0.10 mmol), 0.0016 g of S (0.05 mmol), and 4 g of ODE (90%) was mixed in the three neck flask, bubbled with Ar for 10 min, then heated to 220 °C and reacted under 220 °C for 1 h. The control experiment was carried out exactly the same but without the addition of elemental sulfur.

NMR Measurement. ^1H and ^{13}C NMR measurements were carried out on Bruker 300 and 400 MHz instruments. For quantitatively integration of ^1H spectra to calculate the ODE consumption, a recycle delay time of 60 s was set up to make sure that proton nuclei returned to the equilibrium Boltzmann distribution between pulses.

2-Tetradecylthiophene. ^1H NMR (300 MHz, $CDCl_3$): δ = 7.10 [dd, $^3J(H,H)$ = 5.1 Hz, $^4J(H,H)$ = 1.1 Hz, 1 H, 5-H], 6.91 [dd, $^3J(H,H)$ = 5.1 Hz, $^3J(H,H)$ = 3.4 Hz, 1 H, 4-H], 6.77 [tdd, $^3J(H,H)$ = 3.4 Hz, $^4J(H,H)$ = 1.1 Hz, $^4J(H,H)$ = 1.1 Hz, 1 H, 3-H], 2.81 [t, $^3J(H,H)$ = 7.6 Hz, 2 H, α-CH_2].

Optical Measurements. UV−vis spectra were taken on an HP 8453 UV−visible spectrophotometer. Photoluminescence spectra were measured using a Spex Fluorolog-3 fluorometer.

Transmission Electron Microscopy (TEM). TEM images were taken on a JEOL 100 CX electron microscope using a 100 kV accelerating voltage. CdS nanocrystal was dispersed into toluene or

hexanes solution, then several drops of the solution were added onto a Formvar-coated copper grid, and the grid with the nanocrystals was dried in air.

Fourier Transform Infrared Spectroscopy (FTIR). FTIR spectra were recorded on a Bruker Tensor 27 FT-IR spectrometer at room temperature by directly applying sample onto CaF_2 salt plates.

Gas Chromatography−Mass Spectrometry (GC-MS). The final products after digestion were measured by a Shimadzu QP5050A quadrupole GC/MS system interfaced with a GC-17A gas chromatography. The capillary column used was a Rtx-5 MS 30-m long × 0.25-mm i.d. × 0.25-um film thickness. (Crossbond 5% diphenyl/95% dimethyl polysiloxane, Restek, Bellefonte, PA). Temperature program was 50−300 °C at 20 °C/min. Column flow rate was 1.3 mL/min. Split ratio was 1:1. Acquisition mass range was 50−450 Da.

■ ASSOCIATED CONTENT

Supporting Information. Additional figures and experimental details. This material is available free of charge via the Internet at http://pubs.acs.org.

■ AUTHOR INFORMATION

Corresponding Author
xpeng@zju.edu.cn

■ ACKNOWLEDGMENT

Financial support from the National Science Foundation and Arkansas Biosciences Institute is acknowledged. We are grateful for the critical comments from Dr. J. Hinton.

■ REFERENCES

(1) Murray, C. B.; Kagan, C. R.; Bawendi, M. G. *Annu. Rev. Mater. Sci.* **2000**, *30*, 545.
(2) Peng, X. G. *Nano. Res.* **2009**, *2*, 425.
(3) Peng, X. G. *Chem.—Eur. J.* **2002**, *8*, 335.
(4) Murray, C. B.; Norris, D. J.; Bawendi, M. G. *J. Am. Chem. Soc.* **1993**, *115*, 8706.
(5) Peng, Z. A.; Peng, X. G. *J. Am. Chem. Soc.* **2001**, *123*, 183.
(6) Chen, Y. F.; Kim, M.; Lian, G.; Johnson, M. B.; Peng, X. G. *J. Am. Chem. Soc.* **2005**, *127*, 13331.
(7) Deng, Z. T.; Cao, L.; Tang, F. Q.; Zou, B. S. *J. Phys. Chem. B* **2005**, *109*, 16671.
(8) Steckel, J. S.; Yen, B. K. H.; Oertel, D. C.; Bawendi, M. G. *J. Am. Chem. Soc.* **2006**, *128*, 13032.
(9) Liu, H. T.; Owen, J. S.; Alivisatos, A. P. *J. Am. Chem. Soc.* **2007**, *129*, 305.
(10) Kwon, S. G.; Piao, Y.; Park, J.; Angappane, S.; Jo, Y.; Hwang, N.-M.; Park, J.-G.; Hyeon, T. *J. Am. Chem. Soc.* **2007**, *129*, 12571.
(11) Chen, O.; Chen, X.; Yang, Y. A.; Lynch, J.; Wu, H. M.; Zhuang, J. Q.; Cao, Y. C. *Angew. Chem., Int. Ed.* **2008**, *47*, 8638.
(12) Wang, F. D.; Tang, R.; Buhro, W. E. *Nano Lett.* **2008**, *8*, 3521.
(13) Yordanov, G. G.; Yoshimura, H.; Dushkin, C. D. *Colloid Polym. Sci.* **2008**, *286*, 813.
(14) Wang, F.; Tang, R.; Kao, J. L. F.; Dingman, S. D.; Buhro, W. E. *J. Am. Chem. Soc.* **2009**, *131*, 4983.
(15) Joo, J.; Pietryga, J. M.; McGuire, J. A.; Jeon, S. H.; Williams, D. J.; Wang, H. L.; Klimov, V. I. *J. Am. Chem. Soc.* **2009**, *131*, 10620.
(16) Shen, H. B.; Wang, H. Z.; Li, X. M.; Niu, J. Z.; Wang, H.; Chen, X.; Li, L. S. *Dalton Trans.* **2009**, 10534.
(17) Jung, Y. K.; Kim, J. I.; Lee, J. K. *J. Am. Chem. Soc.* **2010**, *132*, 178.
(18) Allen, P. M.; Walker, B. J.; Bawendi, M. G. *Angew. Chem., Int. Ed.* **2010**, *49*, 760.
(19) Evans, C. M.; Evans, M. E.; Krauss, T. D. *J. Am. Chem. Soc.* **2010**, *132*, 10973.
(20) Cros-Gagneux, A.; Delpech, F.; Nayral, C.; Cornejo, A.; Coppel, Y.; Chaudret, B. *J. Am. Chem. Soc.* **2010**, *132*, 18147.
(21) Owen, J. S.; Chan, E. M.; Liu, H. T.; Alivisatos, A. P. *J. Am. Chem. Soc.* **2010**, *132*, 18206.
(22) Bullen, C.; van Embden, J.; Jasieniak, J.; Cosgriff, J. E.; Mulder, R. J.; Rizzardo, E.; Gu, M.; Raston, C. L. *Chem. Mater.* **2010**, *22*, 4135.
(23) Shen, H. B.; Wang, H. Z.; Chen, X.; Niu, J. Z.; Xu, W. W.; Li, X. M.; Jiang, X. D.; Du, Z. L.; Li, L. S. *Chem. Mater.* **2010**, *22*, 4756.
(24) Karan, N. S.; Mandal, A.; Panda, S. K.; Pradhan, N. *J. Phys. Chem. C* **2010**, *114*, 8873.
(25) Viswanatha, R.; Amenitsch, H.; Santra, S.; Sapra, S.; Datar, S. S.; Zhou, Y.; Nayak, S. K.; Kumar, S. K.; Sarma, D. D. *J. Phys. Chem. Lett.* **2010**, *1*, 304.
(26) Thomson, J. W.; Nagashima, K.; Macdonald, P. M.; Ozin, G. A. *J. Am. Chem. Soc.* **2011**, *133*, 5036.
(27) Xie, R. G.; Li, Z.; Peng, X. G. *J. Am. Chem. Soc.* **2009**, *131*, 15457.
(28) Brus, L. E. *J. Chem. Phys.* **1984**, *80*, 4403.
(29) Yu, W. W.; Peng, X. G. *Angew. Chem., Int. Ed.* **2002**, *41*, 2368.
(30) Yang, Y. A.; Wu, H. M.; Williams, K. R.; Cao, Y. C. *Angew. Chem., Int. Ed.* **2005**, *44*, 6712.
(31) Yu, W. W.; Qu, L. H.; Guo, W. Z.; Peng, X. G. *Chem. Mater.* **2003**, *15*, 2854.
(32) Bellamy, L. J. *The Infra-red Spectra of Complex Molecules*, 3rd ed.; Chapman and Hall: London, 1975.
(33) Nickless, G. *Inorganic Sulphur Chemistry*; Elsevier Pub. Co.: Amsterdam, 1968.
(34) Zabicky, J. *The Chemistry of Alkenes*; Interscience Publishers: London, 1970; Vol. 2.
(35) Oae, S. *Organic Chemistry of Sulfur*; Plenum Press: New York, 1977.
(36) Cotton, F. A. *Advanced Inorganic Chemistry*, 6th ed.; Wiley: New York, 1999.
(37) Li, Z.; Peng, X. *J. Am. Chem. Soc.* **2011**, *133*, 6578.
(38) Timonen, J. V. I.; Seppala, E. T.; Ikkala, O.; Ras, R. H. A. *Angew. Chem., Int. Ed.* **2011**, *50*, 2080.
(39) Cao, Y. C.; Wang, J. H. *J. Am. Chem. Soc.* **2004**, *126*, 14336.
(40) Ouyang, J. Y.; Kuijper, J.; Brot, S.; Kingston, D.; Wu, X. H.; Leek, D. M.; Hu, M. Z.; Ripmeester, J. A.; Yu, K. *J. Phys. Chem. C* **2009**, *113*, 7579.
(41) Zou, Y.; Li, D.; Yang, D. *Nanoscale Res. Lett.* **2010**, *5*, 966.
(42) Pradhan, N.; Reifsnyder, D.; Xie, R. G.; Aldana, J.; Peng, X. G. *J. Am. Chem. Soc.* **2007**, *129*, 9500.
(43) Pradhan, N.; Efrima, S. *J. Am. Chem. Soc.* **2003**, *125*, 2050.
(44) Pradhan, N.; Katz, B.; Efrima, S. *J. Phys. Chem. B* **2003**, *107*, 13843.
(45) Ong, G. L.-P. Purification and surface studies of colloidal semiconductor nanocrystals. Ph.D. Dissertation, University of Arkansas, Fayetteville, AR, 2010.
(46) Davis, R. E.; Nakshbendi, H. F. *J. Am. Chem. Soc.* **1962**, *84*, 2085.
(47) Qu, L. H.; Peng, X. G. *J. Am. Chem. Soc.* **2002**, *124*, 2049.
(48) Li, L. S.; Pradhan, N.; Wang, Y. J.; Peng, X. G. *Nano Lett.* **2004**, *4*, 2261.
(49) Joo, J.; Na, H. B.; Yu, T.; Yu, J. H.; Kim, Y. W.; Wu, F. X.; Zhang, J. Z.; Hyeon, T. *J. Am. Chem. Soc.* **2003**, *125*, 11100.
(50) Watanabe, H.; Ohmori, H. *Talanta* **1979**, *26*, 959.